European Review for Medical and Pharmacological Sciences 2022; 26: 4392-4402

Polydatin alleviates osteoporosis by enhancing the osteogenic differentiation of osteoblasts

Y. YUAN[1], G. FENG[2], J. YANG[3], C. YANG[3], Y.-H. TU[1]

[1]School of Medicine, Tongji University, Shanghai, China
[2]School of Medicine, Ningbo University, Ningbo, Zhejiang, China
[3]Department of Orthopaedics, Hwa Mei Hospital, University of Chinese Academy of Sciences, Ningbo, Zhejiang, China

Abstract. – OBJECTIVE: Osteoporosis is a severe degenerative chronic metabolic bone disease associated with high fracture risk. Polydatin (PD), a major bioactive component of Polygonum cuspidatum, has antioxidant and anti-inflammatory effects. This study investigated the anti-osteoporotic activity of PD in ovariectomized (OVX) mice and elucidated its underlying molecular mechanisms.

SUBJECTS AND METHODS: An osteoporosis mouse model was established using OVX mice. OVX mice were then administered 10 or 40 mg/kg of PD for 60 days. Micro-CT and three-point bending tests were used to determine the therapeutic activities of PD in OVX mice. H&E staining was used to determine whether PD induced hepatorenal toxicity. In addition, the cellular and molecular mechanisms underlying the functionality of PD were elucidated.

RESULTS: Micro-CT results showed that compared to control mice, the bone mass of OVX mice was significantly reduced due to estrogen deficiency; however, PD administration significantly elevated bone mass. Furthermore, PD substantially improved the trabecular microstructure parameters of the femur and enhanced bone strength compared with OVX mice. Hepatorenal toxicity was not observed in liver and kidney samples stained with H&E. PD significantly increased the proliferation of pre-osteoblast MC3T3-E1 cells and upregulated the expression of osteogenic differentiation markers compared to those in controls, as determined by qRT-PCR and western blotting.

CONCLUSIONS: PD exerted a significant anti-osteoporotic effect in OVX mice by promoting osteogenesis. PD has great potential as a therapeutic option for osteoporosis.

Key Words:
Polydatin, Osteoporosis, OVX mice, Trabecular microstructure, Osteogenic differentiation.

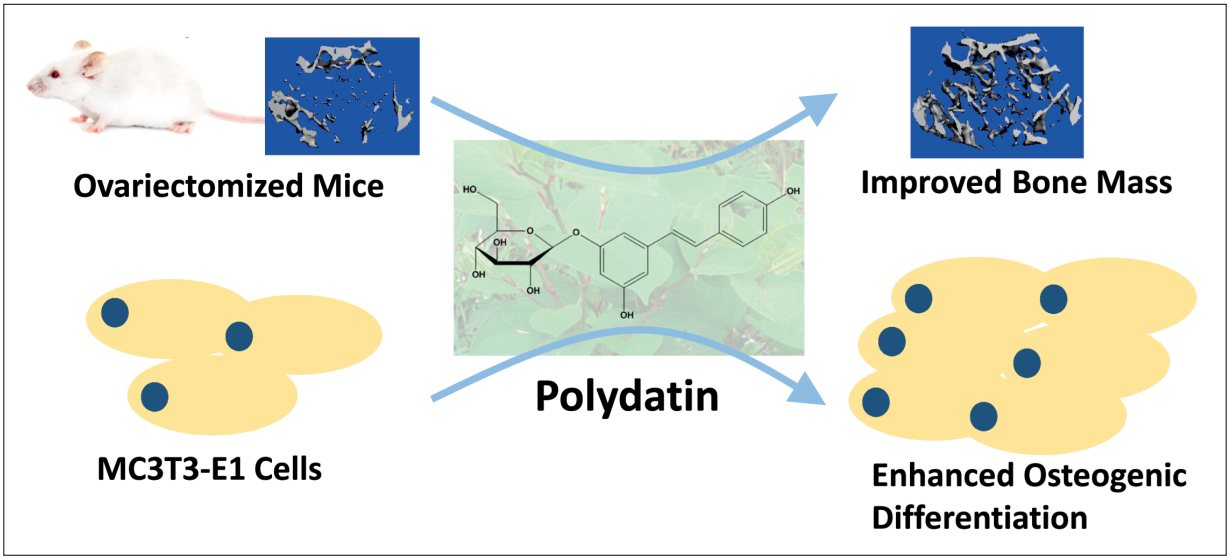

Graphical Abstract. Polydatin, a major bioactive component of *Polygonum cuspidatum*, exerts a significant anti-osteoporotic effect in ovariectomized mice by promoting osteogenesis.

Corresponding Author: Yihui Tu, MD; e-mail: nbjoint@163.com

Introduction

Osteoporosis (OP) is a systemic metabolic bone disease that mainly manifests as decreased bone mass, deterioration of bone microstructure, and reduced bone strength, leading to a significant increase in fracture risk[1]. In mainland China, the overall prevalence of osteoporosis in people over 50 years of age is 30-40% and 10-20% in the female and male populations, respectively[2]. Regardless of the study design and population selection, almost all studies show that the incident rates of osteoporosis in women are higher than in men[2]. This higher incidence in women is associated with postmenopausal osteoporosis, which affects approximately 30% of postmenopausal women in the United States and Europe. Postmenopausal osteoporosis (PMOP) is caused by low estrogen levels after menopause[3]. Although OP is known to be related to sex, age, and steroid use, its specific pathogenesis has not been elucidated[4]. An imbalance in bone remodeling caused by an imbalance in osteoclast and osteoblast differentiation is also a major cause of OP[5-7]. Bone-resorbing osteoclast activity markedly increases with a reduction in estrogen concentration; however, bone-forming osteoblast activity decreases[8,9]. Therefore, the promotion of osteoblast differentiation and restoration of the homeostasis of osteoclasts and osteoblast differentiation may be useful in treating OP.

At present, the main treatment for OP are menopausal hormone therapies (MHT), including estrogen therapy (ET) and estrogen plus progestogen therapy (EPT), which inhibit bone turnover and reduce bone loss[10]. However, MHT may cause serious side effects such as breast cancer, endometrial cancer, and cardiovascular disease[11]. Other FDA-approved osteoporosis-treating drugs include bisphosphonates and the monoclonal antibody denosumab[12]; however, these inhibit bone resorption but do not stimulate new bone formation[13]. Therefore, it is necessary to search for new osteoporosis drugs that are less toxic and can promote bone formation.

Polydatin (PD) is a small natural molecule extracted from the roots of *Polygonum cuspidatum* Sieb. et Zucc. It has been extensively used in traditional Chinese medicine for its expectorant, antipyretic, and analgesic functions[14]. PD also has anti-fibrosis, anti-tumor, anti-oxidation, anti-inflammatory, and anti-bacterial functions, as well as estrogen-like effects[15-17]. PD also has significant protective effects on the lungs, kidneys, liver, and the cardiovascular system[14]. These studies suggest that PD exerts its pharmacological effects by regulating multiple targets and pathways.

In addition to these effects, PD also regulates bone metabolism. By regulating the Wnt/β-catenin pathway[4,18], MAPK pathway[19], and OPG/RANKL ratio, PD improves the osteogenic differentiation of human bone marrow stem cells (hBMSCs)[20]. Therefore, PD has shown promising therapeutic effects against osteoporosis. However, to our knowledge, the potential toxicity of PD *in vivo* has not yet been studied. Moreover, the potential therapeutic effects of PD and the specific mechanisms through which PD exerts its anti-osteoporotic function require further investigation. Therefore, the purpose of this study was to examine the anti-osteoporotic activity of PD in ovariectomized (OVX) mice and in bone-forming-related cells. Our study provides a reliable experimental and theoretical basis for the use of PD in the clinical treatment of osteoporosis.

Subjects and Methods

Animals

Thirty healthy two-month-old female C57BL/6 mice were obtained from the Zhejiang Experimental Animal Center. The experimental animal production license number is SCXK (Zhejiang) 2020-0001. The mice were raised and studied in an individually ventilated cage (IVC) system of specific pathogen-free (SPF) barrier facilities at this center. The license number for experimental animals was SCXK (Zhejiang) 2020-0008. The experimental animals were raised at 22 ± 2°C and 50-60% humidity with a 12-h/12-h light/dark cycle. All animals were provided *ad libitum* access to food and water. All experiments were approved by the Animal Ethics Committee of the Hwa Mei Hospital at the University of Chinese Academy of Sciences.

OVX Mouse Model

After acclimation for one week, all mice were raised for another five weeks before ovary removal. Each mouse was randomly assigned to one of the five groups (n = 6 each): low-concentration group (low), high-concentration group (high), OVX group, sham-operated group (control), and blank group. Subsequently, ovariectomy was performed in the low, high, and OVX groups. After anesthetization by oral administration of 50 mg/kg pentobarbital sodium, bilateral ovaries were removed through an incision in the back. Mice

in the sham-operated group received the same treatment, but partial fat removal was performed instead of ovarian removal. The control group did not undergo any surgical procedures. Mice in the low-dose group were intraperitoneally injected with PD (purity ≥ 98%, Lot No. FY1278S0712; Nantong Feiyu Biotechnology Co., Ltd., Nantong, China) solution at a concentration of 10 mg/kg every two days. Mice in the high-dose group were injected with 40 mg/kg PD every two days. The control, blank, and OVX groups were administered the same volume of saline solution.

The mice were raised for another 60 days and sacrificed via cervical dislocation after anesthesia. The uterine weight and body weight of each group were recorded. The femur and tibiofibula of the lower limbs were rapidly dissected after the removal of the attached muscles and connective tissues. Liver and kidney specimens were rapidly dissected and fixed in 4% paraformaldehyde for further analysis.

Micro-CT Scanning of Femurs

Micro-CT scanning (SkyScan 1174; Bruker, Germany) was used to evaluate femur morphology. The scanning parameters were set as follows: voltage, 50 kV; current, 800 μA; and pixel size, 12 μm (1304×1024 resolution). A 1.5 mm-high area of the distal femur was set as the region of interest (ROI) for 3D reconstruction. NRecon software (Bruker) was used for 3D image reconstruction, and CT-Analyzer software (Bruker) was used for 3D analysis. The trabecular bone parameters, including trabecular separation (Tb.Sp), bone volume per tissue volume (BV/TV), trabecular thickness (Tb.Th), trabecular number (Tb.N), and trabecular pattern factor (Tb.Pf), were also calculated and analyzed.

Mechanical Test

Mice in each group were sacrificed by cervical dislocation after anesthesia with pentobarbital sodium (50 mg/kg). After removing the muscles, fascia, and periosteum, 10 pairs of tibiae were immersed in 0.9% NaCl solution and stored at 4°C. Mechanical testing of the tibiae was conducted using three-point bending tests (TPBTs), as described by Carriero et al[21], using a ZwickiLine material testing machine (BZ2.5/TN1S; ZwickRoell Pte. Ltd., Germany). In accordance with the mechanical test method, the two ends of the sample were supported by two supporters. Vertical pressure (force) was applied at the midpoint between the two ends of the sample. The deflection of the loading point was defined as the vertical displacement of the loading point. As the load increased, the bone flexed and deformed until cracking separated, resulting in a flexural fracture. The testing process was controlled using an interactive computer. The computer collected and stored the data, displayed the load-deflection curve in real-time, and automatically calculated the parameters.

Hematoxylin and Eosin Staining of Liver and Kidney Samples

Liver and kidney tissues were collected and fixed overnight with 4% paraformaldehyde, followed by decalcification. Paraffin slides were heated to 70°C for 15 min in an oven. The slides were automatically stained by H&E using an automated slide stainer (Tissue-Tek Prisma Plus; Sakura, Japan) and covers lipped with a Tissue Tek Automated Coverslipper (Sakura).

Proliferation of RAW264.7 and MC3T3-E1 Cells

Mouse osteoclast RAW264.7 and pre-osteoblast MC3T3-E1 cell lines were obtained from American Type Culture Collection (ATCC, Manassas, VA, USA), cultivated in Dulbecco's Modified Eagle's Medium (DMEM) and α-MEM (Gibco, Waltham, MA, USA), respectively, and supplemented with 10% fetal bovine serum (FBS) (Gibco, origin: New Zealand) and 1% penicillin-streptomycin (Gibco, Waltham, MA, USA) at 5% CO_2 and 37°C.

A Cell Counting Kit-8 (CCK-8; Solarbio, Beijing, China) was used to measure cell proliferation after the addition of PD. MC3T3-E1 cells were induced to differentiate using an osteogenic medium (OM) composed of 10 mM β-glycerophosphate (Solarbio, Beijing, China), 50 μg/mL ascorbic acid (Shanghai Aladdin Biochemical Technology Co. Ltd., Shanghai, China), and 10 nM dexamethasone (Sigma-Aldrich, Shanghai, China). RANKL (Cell Signaling Technology, Danvers, MA, USA) at 50 ng/mL was added to RAW264.7 cells to induce differentiation into osteoclasts. PD was dissolved in anhydrous ethanol (50 mL) to obtain a 10 mM PD-ethanol solution. The PD solution was diluted to a series of concentrations using phosphate-buffered saline (PBS). A total of 5×10^3 cells were seeded into each well of a 96-well plate. After incubation for 24 h, 10 μL of various concentrations of PD solution was added to the wells. The plate was then incubated for a further 48 h, followed by the addition of 10 μL

CCK-8 solution and incubation for another 2 h. A microplate reader (Infinite 200 PRO; TECAN, Männedorf, Switzerland) was used to measure absorbance at 450 nm.

Alizarin Red (AR) Staining

MC3T3-E1 cells were cultivated in OM in 24-well plates. Different concentrations of PD (0, 1, and 100 nM) were added to the wells, followed by continuous cultivation for another 21 d. The wells were rinsed twice with PBS and fixed with 4% PFA (Shanghai Aladdin Biochemical Technology Co., Ltd.) for 30 min. The fixed cells were subjected to AR (Solarbio) staining for 25 min after washing thrice with ddH_2O. Calcium nodules were observed under an optical microscope (Olympus, Tokyo, Japan).

Effect of PD on Osteogenic Differentiation Markers

To characterize cell differentiation, we measured the expression of four osteogenic differentiation markers: osteocalcin (OCN), alkaline phosphatase (ALP), Runx2, and collagen type I alpha 1 chain (COL1A1). MC3T3-E1 cells were cultivated in OM in 6-well plates. After rinsing twice with PBS, fresh OM with or without PD was added to each well. After continuous cultivation for 48 h, the total RNA and protein were extracted for qRT-PCR and western blotting (WB), respectively. Total RNA was extracted using the TransZol UP Plus RNA Kit (TransGen, Beijing, China). The concentration and quality of RNA were determined using a NanoDrop 2000 spectrophotometer (Thermo Fisher Scientific, Waltham, MA, USA). One microgram of RNA was used to synthesize cDNA using EasyScript cDNA Synthesis SuperMix (TransGen). A TranStart qPCR SuperMix Kit (TransGen) was used to quantify the cDNA. The qRT-PCR was conducted using a 7500 Fast PCR system (Applied Biosystems, Waltham, MA, USA). Glyceraldehyde-3-Phosphate Dehydrogenase (GAPDH) was used as an internal control. The relative fold-change in mRNA levels was represented as $2^{-\Delta\Delta Ct}$ compared to that of the control group.

Total protein was extracted after induction with RIPA lysis buffer (Beyotime, Shanghai, China). To inhibit protein degradation, 2 mM PMSF was added to the buffer. The protein concentration in the supernatant was quantified after centrifugation using a bicinchoninic acid assay (BCA) kit (TransGen). Total proteins were separated using 12% Sodium Dodecyl Sulfate–Polyacrylamide Gel Electrophoresis (SDS-PAGE), then transferred to a polyvinylidene difluoride (PVDF) membrane, which was blocked using 5% skim milk. Proteins were detected using primary antibodies against osteogenic differentiation markers. Antibodies against Runx2 (catalog: PA1-41519), OCN (catalog: PA5-86886), and GAPDH (catalog: PA1-988) were purchased from Invitrogen (Carlsbad, CA, USA). Antibodies against ALP (catalog: K108942P) and COL1A1 (catalog: K106404P) were purchased from Solarbio. We incubated the membranes with HRP-conjugated secondary antibodies (Solarbio) after three washes with Tris-Buffered Saline and Tween-20 (TBST). Bands on the PVDF membranes were visualized using an eECL WB kit (CWBIO, Beijing, China). Western blot images were captured using ChampChemi software (Sage, Beijing, China). ImageJ software was used to determine the protein level based on the GAPDH level as an endogenous control.

Statistical Analysis

Statistical analyses were performed using SPSS 26.0 (SPSS Corp., IBM, Armonk, NY, USA). Data are expressed as the mean ±SD. One-way ANOVA was used for statistical analysis. A p-value of less than 0.05 was considered to be statistically significant.

Results

Changes in Body Weight and Uterine Weight After PD Injection

As shown in Figure 1A, after 60 days of treatment, OVX mice gained significantly more body weight than mice in the blank and control groups ($p < 0.001$). Notably, the weight gain in OVX mice was reversed after treatment with PD. Low and high concentrations of PD significantly inhibited weight gain in OVX mice. PD at high doses contributed to an 11.4% reduction in weight gain compared with the OVX group (Figure 1A). No significant differences in body weights were observed between the blank and control groups.

In contrast to the observed weight gain, the uterine index (uterine index = wet uterine weight (mg)/body weight (g)) was significantly lower in OVX mice than in blank and control mice ($p < 0.001$, Figure 1B). However, compared to the OVX group, low and high concentrations of PD markedly increased the uterine index ($p < 0.001$). The ability of high PD concentrations to increase the uterine index was significantly greater than that of low PD concentrations ($p < 0.001$).

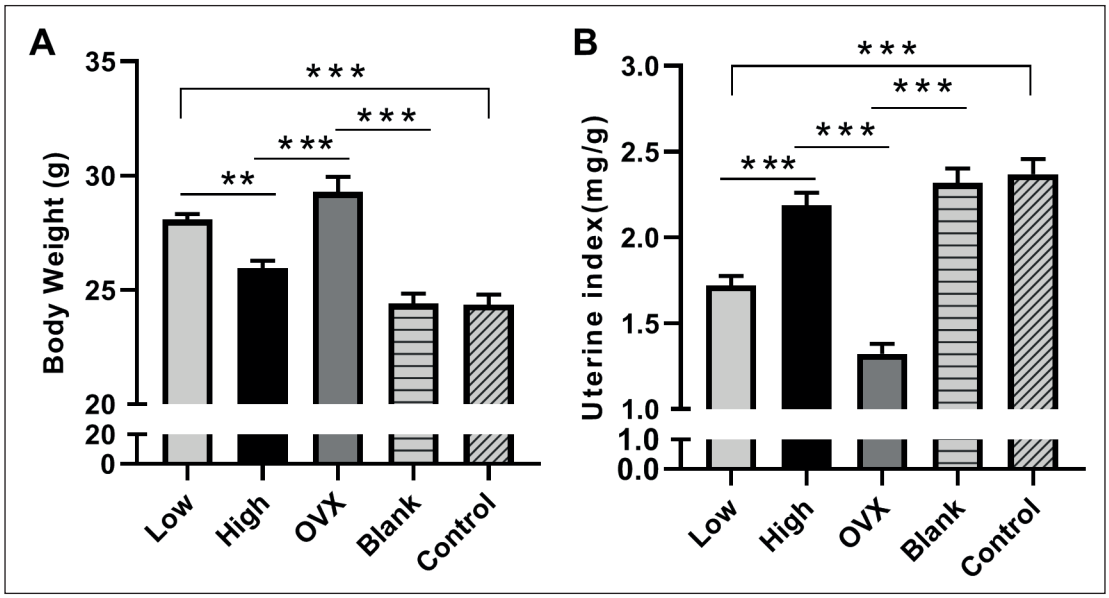

Figure 1. Determination of body weight and uterine index. **A-B**, At the end of the experiment, the mice were weighed (**A**) and sacrificed. The uterus was then removed, and the uterine index was calculated (**B**). Uterine index = wet uterine weight (mg)/body weight (g). Data are expressed as mean ± SD, and one-way ANOVA was used for statistical analysis, $^{**}p < 0.01$, $^{***}p < 0.001$.

Micro-CT Scanning

To investigate whether PD reduces estrogen deficiency-related bone loss, distal femurs from PD-treated mice were analyzed using micro-CT. The results demonstrated that trabecular bone mass in the OVX group was significantly reduced compared to that in the control group. PD administration significantly improved the bone mass in OVX mice, regardless of the concentration used. Mice in the high PD group exhibited greater bone mass than those in the low group (Figure 2A). Collectively, these results indicate that PD administration reduces bone loss.

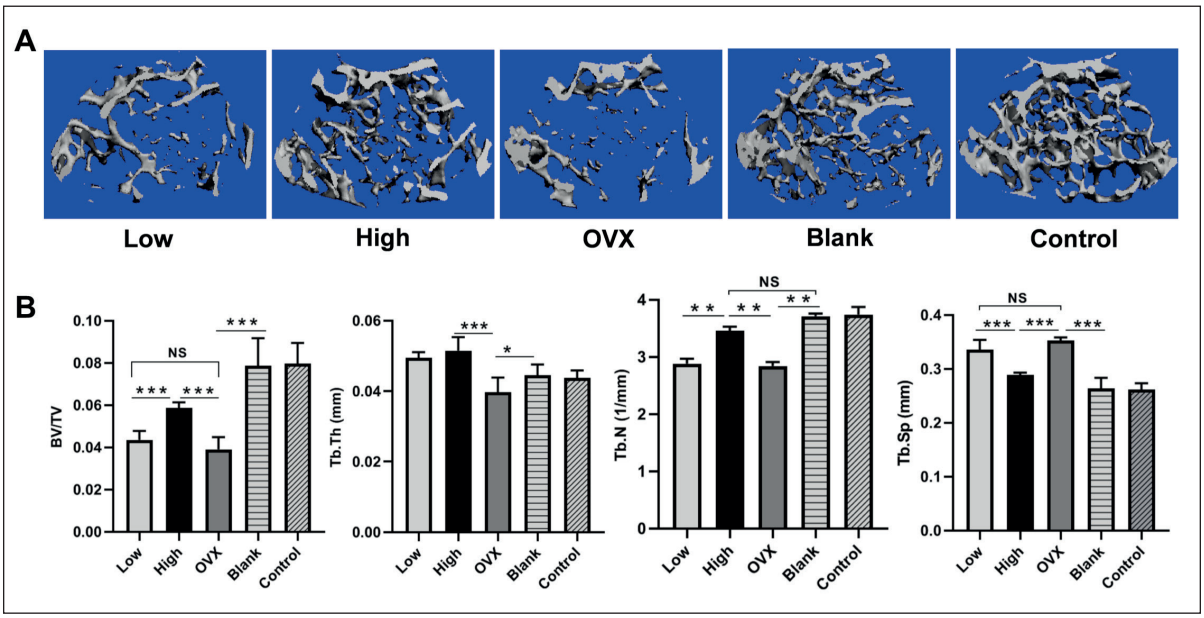

Figure 2. Micro-CT analysis of microstructures in the femur. **A,** Representative images of the 3D reconstruction of femurs from all groups. **B,** Micro-CT analysis of Tb.N, BV/TV, Tb.Th, and Tb.Sp. Data are presented as mean ± SD, n = 3 rats for each group. One-way ANOVA was used for analysis, $^{*}p < 0.05$, $^{**}p < 0.01$, and $^{***}p < 0.001$. NS, not significant.

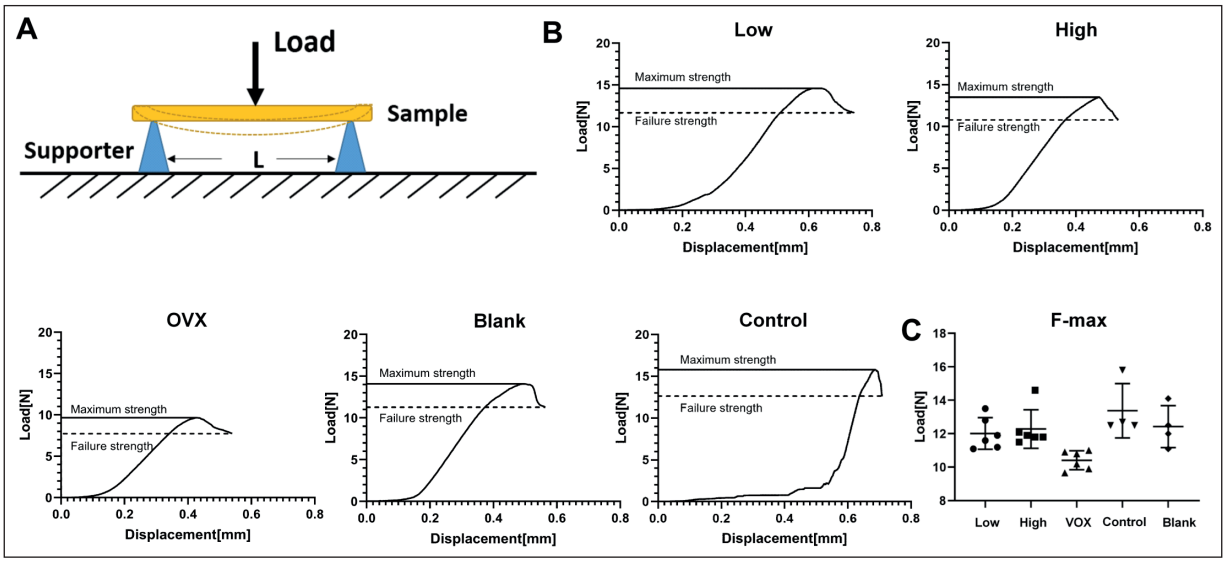

Figure 3. Assessment of mechanical properties of tibiae. **A,** Schematic diagram of the three-point bending test (TPBT) using ZwickiLine materials testing machine. 'L' represents span. **B,** TPBT was utilized to assess the stiffness of tibiae in all groups. The resulting data are plotted as load *vs.* displacement. **C,** The load reaching the fracture point in all groups.

We also determined the parameters used to characterize the trabecular microstructure (Figure 2B). OVX mice exhibited lower BV/TV, Tb.N, and Tb.Th values but a higher Tb.Sp value ($p < 0.001$) than those in the blank and control groups. In contrast to OVX mice, PD-treated mice also showed improved trabecular parameters. Mice in the high PD group exhibited significantly higher BV/TV, Tb.N, and Tb.Th values and a lower Tb.Sp value than mice in the OVX group. These results suggest that PD had a positive effect on osteogenesis.

Mechanical Analysis

To evaluate the effect of estrogen deficiency and PD administration on bone strength and mechanical properties, a TPBT was performed using the tibia, as described by Carriero et al[21] (Figure 3A). Two key parameters were obtained from the TPBT: maximum load on the tibia and load on the tibial fracture. The maximum load on the tibia and the load on the tibial fracture were markedly lower in OVX mice than in the blank and control mice (Figure 3B, C). PD, regardless

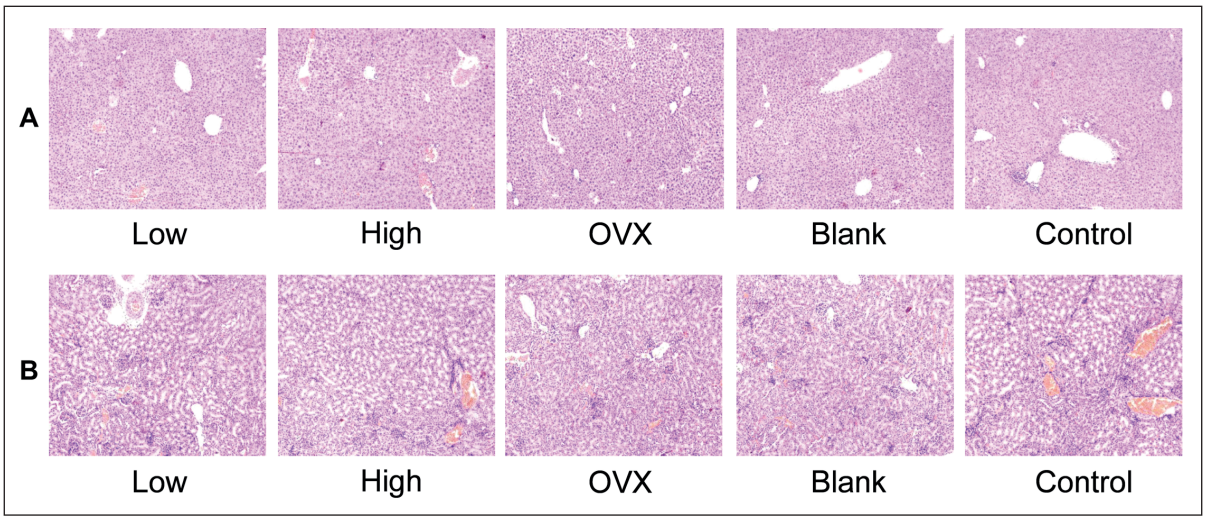

Figure 4. H&E staining of liver and kidney samples isolated from mice. **A-B,** Representative images of liver tissue (**A**) and kidney tissue (**B**) isolated from mice in all groups (100 × magnification). At the end of the experiment, the liver and kidney tissues from each group were dissected and stained with H&E.

of concentration, significantly elevated these two parameters. There was no statistical difference in the maximum load on the tibia and load on the tibial fracture among the low PD, high PD, control, and blank groups. These data show that the administration of PD substantially improved the mechanical strength of the tibia in OVX mice.

H&E Staining

H&E staining of the kidney and liver tissues was conducted at the end of the experiments to determine whether PD had toxic effects on mice. The liver tissue showed that the lobules of mice in each group were clearly structured, and cells were neatly arranged without vacuoles, hemorrhage, necrosis, or inflammatory cell infiltration (Figure 4A). The renal tissue showed clear structures of the renal tubules and glomeruli, with no edema observed in the renal interstitium. The structure of the renal cortex was also complete, and no inflammatory cell infiltration, hyperemia, or necrosis was observed (Figure 4B). These results suggest that PD is safe for mice, with no toxicity to the liver and kidneys.

Effect of PD on Cell Proliferation

To further clarify the mechanisms underlying the anti-osteoporotic effects of PD, we measured cell proliferation. To confirm the effects of PD on cell proliferation, we used the pre-osteoblast MC3T3-E1 cell line and RAW264.7 cells that had been converted into osteoclasts by RANKL. Compared with the control cells, PD treatment significantly increased the proliferation of MC3T3-E1 cells. At higher concentrations, PD more strongly promoted cell proliferation. Indeed, compared with untreated cells, PD significantly promoted the proliferation of MC3T3-E1 cells even at a dose of 0.1 nM ($p < 0.001$). At a PD concentration of 100 nM, cell proliferation was approximately 7-fold higher than that at 0 nM. However, no significant differences in the proliferation were observed between the 100 nM and 250 nM treatment groups (Figure 5A). In contrast, the proliferation of RAW264.7 cells was significantly inhibited by PD treatment only when the concentration of PD reached 1 nM, resulting in a reduction of approximately 20% compared to the control. Notably, increasing the concentration of PD above 1 nM did not inhibit osteoclast proliferation (Figure 5B). Our results indicate that PD alleviates osteoporosis by promoting osteoblast proliferation and inhibiting osteoclast proliferation.

Table I. Primers used in qRT-PCR.

Name	Sequence
OCN-F	AGGAGGGCAGCGAGGTAG
OCN-R	GAAAGCCGATGTGGTCAGC
ALP-F	GCAGTATGAATTGAATCGGAACAAC
ALP-R	ATGGCCTGGTCCATCTCCAC
COL1A1-F	GACATGTTCAGCTTTGTGGACCTC
COL1A1-R	GGGACCCTTAGGCCATTGTGTA
Runx2-F	GAACCAAGAAGGCACAGACAGA
Runx2-R	GGCGGGACACCTACTCTCATAC
GAPDH-F	TGTCCGTCGTGGATCTGA
GAPDH-R	TTGCTGTTGAAGTCGCAGGAG

Effect of PD on Osteogenic Differentiation

To further investigate the ability of PD to promote osteoblast differentiation, we performed alizarin red (AR) staining. The results demonstrated that PD enhanced mineralization capacity in a dose-dependent manner: more calcium nodules were found in PD-treated cells than in untreated cells, even at a concentration of 1 nM (Figure 5C).

To further investigate the possible molecular mechanism by which PD contributes to bone growth, we examined the expression of osteogenic differentiation-related genes in MC3T3-E1 cells using qRT-PCR and WB. PD promoted the expression of osteogenic differentiation markers in a dose-dependent manner. Compared to untreated cells, an increase in PD concentration increased the expression levels of OCN, ALP, COL1A1, and Runx2 genes during osteogenic differentiation (Figure 6A), even at a concentration of 1 nM. WB results showed similar increases in protein levels (Figure 6B, C). Taken together, these results indicate that PD enhances osteogenesis by promoting the expression of key osteogenic markers.

Discussion

Natural medicines have diverse chemical structures and biological activities and have gradually become a huge resource pool for drug research and development[22]. Many herbal extracts have been shown to significantly enhance the differentiation of osteoblasts and hBMSCs[4,23]. PD is an active ingredient in traditional Chinese medicine and is extracted from *Polygonum cuspidatum*. PD is also found in many types of vegetables and fruits such as peanuts, hop cones, and grapes[14,24]. PD is the precursor to resveratrol and has a wide range of physiological actions[25], including therapeutic effects in diseases such as non-alcoholic steatohepatitis[26],

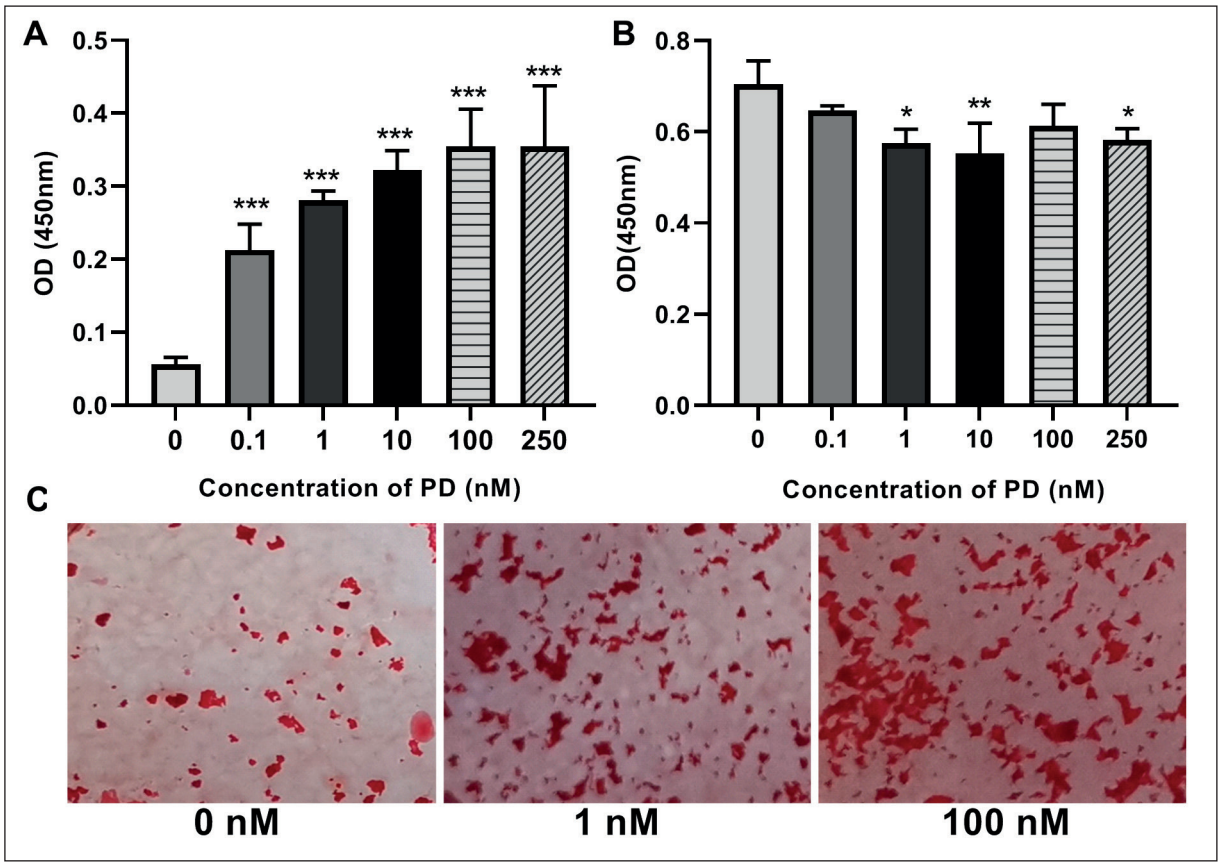

Figure 5. Effects of PD on cell proliferation. **A-B,** The effects of PD on the proliferation of pre-osteoblast MC3T3-E1 cells (**A**) and RANKL-induced RAW264.7 osteoclast cells (**B**). Cells were seeded in a 96-well plate at a density of 5×10^3 cells/well. Ten milliliters of a series of concentrations of PD solutions were added to the wells. After incubation for 48 h, the proliferation of cells was assessed using the CCK-8 method. **C,** Representative images of AR staining (100 × magnification). The MC3T3-E1 cells were continuously stimulated by PD (0, 1, and 100 nM) in an osteogenic medium, followed by AR staining. Data are expressed as mean ± SD and one-way ANOVA was used for analysis, $^{*}p < 0.05$, $^{**}p < 0.01$, and $^{***}p < 0.001$.

traumatic brain injury[27], rheumatoid arthritis[28], and osteosarcoma[29]. PD also promotes the osteogenic differentiation of dental bud stem cells (DBSCs)[24] and hBMSCs[4]. However, relatively few studies have explored the effects of PD on osteoblasts or the therapeutic effects of PD on osteoporosis.

Postmenopausal osteoporosis is associated with estrogen deficiency caused by the deterioration of ovarian function in postmenopausal women and is one of the most common causes of bone mass loss[30]. Osteoporosis induced by OVX in mice is a common and reliable animal model that can simulate postmenopausal osteoporosis symptoms[31]. In this study, we successfully established an OVX mouse model and administered different concentrations of PD over 60 days to determine whether PD had a therapeutic effect on OVX mice.

Micro-CT is an effective method for evaluating the 3D microstructure of bone and can be used to understand its biomechanical properties and the effects of drug intervention[32]. BV/TV, Tb.N, Tb.Th, and Tb.Sp are the most commonly used indices for evaluating the microstructure of the bone trabeculae. When bone catabolism is greater than bone anabolism, as in osteoporosis, bone trabecular perforation and disappearance occur, resulting in a reduction in Tb.N and an increase in Tb.Sp[33]. In this study, BV/TV, Tb.N, and Tb.Th were significantly decreased in OVX mice; however, the value of Tb.Sp was increased compared with those in blank and control mice. This is consistent with the trabecular bone characteristics observed in patients with osteoporotic fractures by Tamimi et al[34]. Our findings revealed that PD reversed the destruction of the trabecular microstructure. PD administration also significantly improved trabecular parameters compared with OVX mice, indicating that PD influenced the

prevention of osteoporosis. However, the optimal concentration of PD has not yet been determined and requires further study.

Trabecular microarchitecture plays an essential role in bone strength, especially in Tb.N and connectivity[35]. The TPBT is a method for measuring and evaluating bone mechanical properties and can be used to characterize the brittleness of bone[36]. To the best of our knowledge, this is the first study to evaluate the effect of PD on bone strength. According to our mechanical data, the stiffness of the tibia in OVX mice was significantly reduced compared with that of the blank and control mice, proving that the osteoporosis model was successful. During osteoporosis, bone strength decreases, and fractures are more likely to occur[37]. PD, regardless of concentration, significantly improved the stiffness of the tibia and mitigated the symptoms of osteoporosis, compared with those of the OVX mice. This enhancement of bone strength may be related to the improvement in trabecular microstructure[34,35]. Combining the micro-CT and TPBT data, we conclude that PD significantly attenuates bone loss and alleviates osteoporosis in OVX mice.

We also explored the underlying mechanism by which PD exerts its anti-osteoporotic effect. Our results demonstrated that PD significantly improved osteoblast proliferation and inhibited osteoclast proliferation. PD increased the expression levels of the osteogenic differentiation markers COL1A1, OCN, ALP, and Runx2, indicating an improvement in bone formation. Our observations are in line with those of previous studies showing that PD (10, 30, and 100 μM) significantly increases the proliferation of hBMSCs and enhances the expression of Runx2, OCN, and COL1A1 during hBMSC osteogenesis[4,38]. In contrast, we found that 1 nM PD was sufficient to stimulate osteoblast differentiation and marker expression, which is much lower than the 10 μM concentration used previously. However, compared to 100 nM PD, 250 nM PD did not further stimulate osteoblast proliferation. These differences in PD concentration effects may be due to the type of cell being studied. Consistent with our

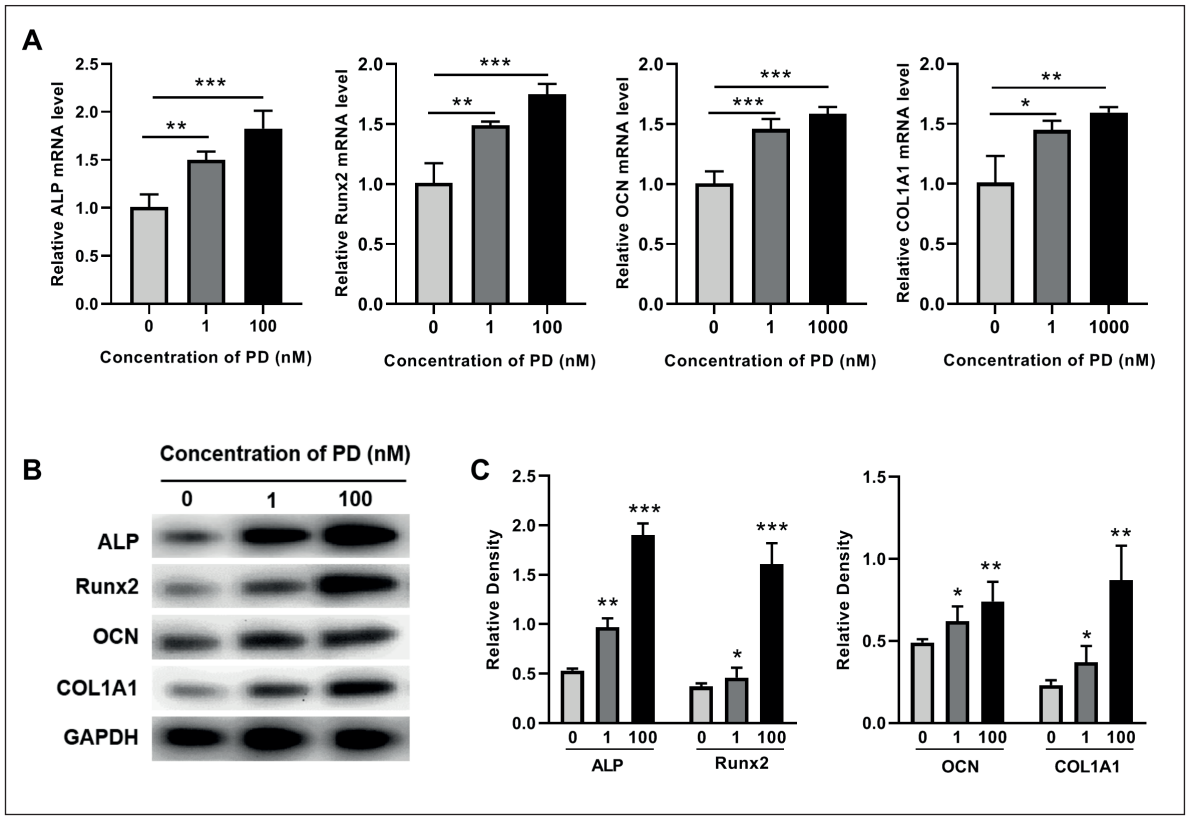

Figure 6. Effects of PD on osteogenic differentiation markers. **A-B,** PD upregulated the expression levels of markers for osteogenic differentiation, including OCN, ALP, COL1A1, and Runx2, in MC3T3-E1 cells, as determined by qRT-PCR (**A**) and WB (**B**). **C,** Semi-quantitative method to determine protein levels based on densitometry, with GAPDH as a control. Data are expressed as mean ± SD and one-way ANOVA was used for analysis, $^{*}p < 0.05$, $^{**}p < 0.01$, and $^{***}p < 0.001$.

data, a study conducted by Di Benedetto et al[24] found that 0.1 μM (100 nM) PD consistently elevated the osteogenic differentiation of DBSCs, while 1 μM PD slightly inhibited cell viability. Although different cell types respond differently to PD, these studies confirm that PD enhances osteogenic differentiation.

In addition, PD employs other mechanisms to exert bone protective effects. Chen et al[39] reported that PD protects BMSCs isolated from rats against apoptosis through anti-oxidation. PD also ameliorates arthritis symptoms in rats by exerting anti-inflammatory and antioxidant effects[28]. Lastly, PD can be applied in the treatment of ankylosing spondylitis, as it induces autophagy and apoptosis in fibroblasts[40].

To use a therapeutic agent clinically, considering its safety is crucial. Although PD has been used in traditional Chinese medicine for a long time, its toxicological effects have not been reported[14]. Therefore, we performed H&E staining of kidney and liver tissues to determine whether PD causes damage to the liver and kidneys. We found that the morphologies of the liver and kidney in PD-treated mice, even those treated with high concentrations, were not significantly different from those in control mice, indicating that PD use was safe. Taken together, these findings support the clinical applications of PD.

Conclusions

PD exhibited significant anti-osteoporotic activity in OVX mice. We demonstrated that PD administration improved the trabecular microstructure and enhanced bone strength in OVX mice. Cytological and molecular mechanistic studies revealed that PD promoted the expression of bone formation-related markers, elevated the proliferation of osteoblasts, and inhibited the proliferation of osteoclasts. H&E staining of the kidney and liver tissues confirmed the safety of PD for *in vivo* applications. Although our results are preliminary, they lay the foundation for further research on anti-osteoporotic drugs and their pharmacological effects.

Acknowledgements

This study was supported by the Medical and Health Science and Technology Project of Zhejiang Province (No. 2020KY264). For the English language editing, we would like to thank Editage (www.editage.cn).

Ethical Approval

All experiments were approved by the Animal Ethics Committee of the Hwa Mei Hospital at the University of Chinese Academy of Sciences.

Conflicts of Interest

The authors declare no conflicts of interest.

References

1) Johnston CB, Dagar M. Osteoporosis in Older Adults. Med Clin N Am 2020; 104: 873-884.
2) Yu F, Xia W. The epidemiology of osteoporosis, associated fragility fractures, and management gap in China. Arch Osteoporos 2019; 14: 32.
3) Ji MX, Yu Q. Primary osteoporosis in postmenopausal women. Chronic Dis Transl Med 2015; 1: 9-13.
4) Shen YS, Chen XJ, Wuri SN, Yang F, Pang FX, Xu LL, He W, Wei QS. Polydatin improves osteogenic differentiation of human bone mesenchymal stem cells by stimulating TAZ expression via BMP2-Wnt/beta-catenin signaling pathway. Stem Cell Res Ther 2020; 11: 204.
5) Chen X, Wang Z, Duan N, Zhu G, Schwarz EM, Xie C. Osteoblast-osteoclast interactions. Connect Tissue Res 2018; 59: 99-107.
6) Kaur M, Nagpal M, Singh M. Osteoblast-n-osteoclast: making headway to osteoporosis treatment. Curr Drug Targets 2020; 21: 1640-1651.
7) Föger-Samwald U, Dovjak P, Azizi-Semrad U, Kerschan-Schindl K, Pietschmann P. Osteoporosis: Pathophysiology and therapeutic options. EXCLI J 2020; 19: 1017-1037.
8) Drake MT, Clarke BL, Lewiecki EM. The Pathophysiology and Treatment of Osteoporosis. Clin Ther 2015; 37: 1837-1850.
9) Rachner TD, Khosla S, Hofbauer LC. Osteoporosis: now and the future. Lancet 2011; 377: 1276-1287.
10) Fait T. Menopause hormone therapy: latest developments and clinical practice. Drugs Context 2019; 8: 212551.
11) McNeil M. Menopausal hormone therapy: understanding long-term risks and benefits. JAMA 2017; 318: 911-913.
12) Tański W, Kosiorowska J, Szymańska-Chabowska A. Osteoporosis - risk factors, pharmaceutical and non-pharmaceutical treatment. Eur Rev Med Pharmacol Sci 2021; 25: 3557-3566.
13) Russow G, Jahn D, Appelt J, Märdian S, Tsitsilonis S, Keller J. Anabolic Therapies in Osteoporosis and Bone Regeneration. Int J Mol Sci 2019; 20: 83.
14) Du QH, Peng C, Zhang H. Polydatin: A review of pharmacology and pharmacokinetics. Pharm Biol 2013; 51: 1347-1354.
15) Jiang J, Chen Y, Dong T, Yue M, Zhang Y, An T, Zhang J, Liu P, Yang X. Polydatin inhibits hepato-

cellular carcinoma via the AKT/STAT3-FOXO1 signaling pathway. Oncol Lett 2019; 17: 4505-4513.

16) Yousef AI, Shawki HH, El-Shahawy AA, El-Twab SMA, Abdel-Moneim A, Oishi H. Polydatin mitigates pancreatic β-cell damage through its antioxidant activity. Biomed Pharmacother 2021; 133: 111027.

17) Zhao X, Yang Y, Yu H, Wu W, Sun Y, Pan Y, Kong L. Polydatin inhibits ZEB1-invoked epithelial-mesenchymal transition in fructose-induced liver fibrosis. J Cell Mol Med 2020; 24: 13208-13222.

18) Chen XJ, Shen YS, He MC, Yang F, Yang P, Pang FX, He W, Cao YM, Wei QS. Polydatin promotes the osteogenic differentiation of human bone mesenchymal stem cells by activating the BMP2-Wnt/beta-catenin signaling pathway. Biomed Pharmacother 2019; 112: 108746.

19) Lin Z, Xiong Y, Hu Y, Chen L, Panayi AC, Xue H, Zhou W, Yan C, Hu L, Xie X, Sun Y, Mi B, Liu G. Polydatin ameliorates osteoporosis via suppression of the mitogen-activated protein kinase signaling pathway. Front Cell Dev Biol 2021; 9: 730362.

20) Zhou QL, Qin RZ, Yang YX, Huang KB, Yang XW. Polydatin possesses notable antiosteoporotic activity via regulation of OPG, RANKL and betacatenin. Mol Med Rep 2016; 14: 1865-1869.

21) Carriero A, Bruse JL, Oldknow KJ, Millan JL, Farquharson C, Shefelbine SJ. Reference point indentation is not indicative of whole mouse bone measures of stress intensity fracture toughness. Bone 2014; 69: 174-179.

22) Orlikova B, Legrand N, Panning J, Dicato M, Diederich M. Anti-inflammatory and anticancer drugs from nature. Cancer Treat Res 2014; 159: 123-143.

23) Mukudai Y, Kondo S, Koyama T, Li C, Banka S, Kogure A, Yazawa K, Shintani S. Potential anti-osteoporotic effects of herbal extracts on osteoclasts, osteoblasts and chondrocytes in vitro. BMC Complement Altern Med 2014; 14: 29.

24) Di Benedetto A, Posa F, De Maria S, Ravagnan G, Ballini A, Porro C, Trotta T, Grano M, Muzio LL, Mori G. Polydatin, natural precursor of resveratrol, promotes osteogenic differentiation of mesenchymal stem cells. Int J Med Sci 2018; 15: 944-952.

25) Chen G, Yang Z, Wen D, Guo J, Xiong Q, Li P, Zhao L, Wang J, Wu C, Dong L. Polydatin has anti-inflammatory and antioxidant effects in LPS-induced macrophages and improves DSS-induced mice colitis. Immun Inflamm Dis 2021; 9: 959-970.

26) Chen X, Chan H, Zhang L, Liu X, Ho IHT, Zhang X, Ho J, Hu W, Tian Y, Kou S, Chan CS, Yu J, Wong SH, Gin T, Chan MTV, Sun X, Wu WKK. The phytochemical polydatin ameliorates non-alcoholic steatohepatitis by restoring lysosomal function and autophagic flux. J Cell Mol Med 2019; 23: 4290-4300.

27) Gu Z, Li L, Li Q, Tan H, Zou Z, Chen X, Zhang Z, Zhou Y, Wei D, Liu C, Huang Q, Maegele M, Cai D, Huang M. Polydatin alleviates severe traumatic brain injury induced acute lung injury by inhibiting S100B mediated NETs formation. Int Immunopharmacol 2021; 98: 107699.

28) Kamel KM, Gad AM, Mansour SM, Safar MM, Fawzy HM. Novel anti-arthritic mechanisms of polydatin in complete freund's adjuvant-induced arthritis in rats: involvement of IL-6, STAT-3, IL-17, and NF-κB. Inflammation 2018; 41: 1974-1986.

29) Jiang CQ, Ma LL, Lv ZD, Feng F, Chen Z, Liu ZD. Polydatin induces apoptosis and autophagy via STAT3 signaling in human osteosarcoma MG-63 cells. J Nat Med 2020; 74: 533-544.

30) Faienza MF, Ventura A, Marzano F, Cavallo L. Postmenopausal osteoporosis: the role of immune system cells. Clin Dev Immunol 2013; 2013: 575936.

31) Qi M, Zhang L, Ma Y, Shuai Y, Li L, Luo K, Liu W, Jin Y. Autophagy maintains the function of bone marrow mesenchymal stem cells to prevent estrogen deficiency-induced osteoporosis. Theranostics 2017; 7: 4498-4516.

32) Jiang Y, Zhao J, Liao EY, Dai RC, Wu XP, Genant HK. Application of micro-CT assessment of 3-D bone microstructure in preclinical and clinical studies. J Bone Miner Metab 2005; 23: 122-131.

33) Mc Donnell P, Mc Hugh PE, O' Mahoney D. Vertebral osteoporosis and trabecular bone quality. Ann Biomed Eng 2007; 35: 170-189.

34) Tamimi I, Cortes ARG, Sánchez-Siles J-M, Ackerman JL, González-Quevedo D, García Á, Yaghoubi F, Abdallah M-N, Eimar H, Alsheghri A, Laurenti M, Al-Subaei A, Guerado E, García-de-Quevedo D, Tamimi F. Composition and characteristics of trabecular bone in osteoporosis and osteoarthritis. Bone 2020; 140: 115558.

35) Legrand E, Chappard D, Pascaretti C, Duquenne M, Krebs S, Rohmer V, Basle MF, Audran M. Trabecular bone microarchitecture, bone mineral density, and vertebral fractures in male osteoporosis. J Bone Miner Res 2000; 15: 13-19.

36) Deckard C, Walker A, Hill BJF. Using three-point bending to evaluate tibia bone strength in ovariectomized young mice. J Biol Phys 2017; 43: 139-148.

37) Hart NH, Nimphius S, Rantalainen T, Ireland A, Siafarikas A, Newton RU. Mechanical basis of bone strength: influence of bone material, bone structure and muscle action. J Musculoskelet Neuron Interact 2017; 17: 114-139.

38) Chen XJ, Shen YS, He MC, Yang F, Yang P, Pang FX, He W, Cao YM, Wei QS. Polydatin promotes the osteogenic differentiation of human bone mesenchymal stem cells by activating the BMP2-Wnt/β-catenin signaling pathway. Biomed Pharmacother 2019; 112: 108746.

39) Chen M, Hou Y, Lin D. Polydatin protects bone marrow stem cells against oxidative injury: involvement of Nrf 2/ARE pathways. Stem Cells Int 2016; 2016: 9394150.

40) Ma C, Wen B, Zhang Q, Shao P, Gu W, Qu K, Shi Y, Wang B. Polydatin regulates the apoptosis and autophagy of fibroblasts obtained from patients with ankylosing spondylitis. Biol Pharm Bull 2019; 42: 50-56.